Published in final edited form as:
Cancer Res. 2008 August 15; 68(16): 6643–6651. doi:10.1158/0008-5472.CAN-08-0850.

Glycogen Synthase Kinase 3 inhibition Induces Glioma Cell Death through c-MYC, NF-κB and Glucose Regulation

Svetlana Kotliarova, **Sandra Pastorino**, **Lara C. Kovell**, **Yuri Kotliarov**, **Hua Song**, **Wei Zhang**, **Rolanda Bailey**, **Dragan Maric**[1], **Jean Claude Zenklusen**, **Jeongwu Lee**, and **Howard A. Fine**

Neuro-Oncology Branch, National Cancer Institute, Bethesda, MD, USA

1*National Institute of Neurological Disorder and Stroke, National Institutes of Health, Bethesda, MD, USA*

Abstract

Glycogen synthase kinase-3 (GSK3), a serine/threonine kinase, is involved in diverse cellular processes ranging from nutrient and energy homeostasis to proliferation and apoptosis. Its role in glioblastoma multiforme (GBM) has yet to be elucidated.

We identified GSK3 as a regulator of GBM cell survival using microarray analysis, small molecule and genetic inhibitors of GSK3 activity. Various molecular and genetic approaches were then employed to dissect out the molecular mechanisms responsible for GSK3 inhibition-induced cytotoxicity.

We demonstrate that multiple small molecular inhibitors of GSK3 activity and genetic down-regulation of GSK3α/β significantly inhibit glioma cell survival and clonogenicity. The potency of the cytotoxic effects is directly correlated with decreased enzyme activity-activating phosphorylation of GSK3α/β Y276/Y216 and with increased enzyme activity-inhibitory phosphorylation of GSK3α S21. Inhibition of GSK3 activity results in c-MYC activation leading to the induction of Bax, Bim, DR4/DR5 and TRAIL expression and subsequent cytotoxicity. Additionally, down-regulation of GSK3 activity results in alteration of intracellular glucose metabolism resulting in dissociation of hexokinase-II (HKII) from the outer mitochondrial membrane with subsequent mitochondrial destabilization. Finally, inhibition of GSK3 activity causes a dramatic decrease in intracellular nuclear factor-kappa B (NF-κB) activity.

Inhibition of GSK3 activity results in c-MYC dependent glioma cell death through multiple mechanisms, all of which converge on the apoptotic pathways. GSK3 may therefore be an important therapeutic target for gliomas. Future studies will further define the optimal combinations of GSK3 inhibitors and cytotoxic agents for use in gliomas and other cancers.

Keywords

GSK3; NF-κB; c-MYC; glucose

Corresponding author: Howard A. Fine, M.D. Neuro-Oncology Branch National Cancer Institute Room 225 The Bloch Building (#82) 9030 Old Georgetown Rd. Bethesda, MD 20892 Tele# 301/402−6383 Fax# 301/480−2246 hfine@mail.nih.gov.

INTRODUCTION

Glioblastomas (GBM) are among the most lethal tumors. New therapeutic approaches utilizing novel molecular targets are clearly needed. In the course of conducting a clinical trial of enzastaurin (LY317615.HCl), a new small molecule inhibitor of protein kinase C-beta (PKCβ)([1]), we noted a number of impressive radiographic responses in patients with recurrent glioblastomas, consistent with a primary cytotoxic mechanism of action rather than, or in addition to, a pure anti-angiogenic mechanism of the drug (2). While attempting to elucidate the apparent cytotoxic activity of enzastaurin against gliomas, we discovered that the alpha and beta forms of GSK3 were targets of the drug in addition to its primary target, PKCβ, (Figure S1). In this study we therefore evaluated whether GSK3 may be a potentially new therapeutic target in gliomas.

GSK3 was initially identified over 25 years ago as a protein kinase that phosphorylated and inactivated glycogen synthase (GYS) (3), the final enzyme in glycogen biosynthesis. Recently it has been recognized as a key component of a diverse range of cellular functions essential for survival (for reviews see (4, [5]). The role of GSK3 in the regulation of apoptosis is controversial. GSK3β knockout mice are embryonically lethal, and mouse embryonic fibroblasts (MEFs) derived from these embryos are sensitized to apoptosis (6). However, this observation appears to contradict the finding that overexpression of GSK3 is sufficient to induce apoptosis (7). A recent report has demonstrated that GSK3 is a pro-survival factor in pancreatic tumor cells, partly through its ability to regulate the NF-κB pathway (8). These data are consistent with the recent demonstration that GSK3β can regulate NF-κB stability and activity (6, [9]). Finally, new experimental evidence suggests that GSKβ inhibition can promote Bax-mediated apoptosis in colorectal cancer cells (10). These data confirm the complex role of GSK3 in apoptosis and demonstrate that the biological outcome of GSK3 signaling is cell type and tissue context-dependent.

Little is currently known regarding the significance of GSK3 to glioma cell survival. We therefore sought to evaluate the role of GSK3 in glioma cell survival, proliferation and tumorigenicity both *in vitro* and *in vivo* and on the mechanistic consequences of inhibiting GSK3 activity. Our data point to GSK3 as a potentially attractive new target for human glioma therapy.

MATERIALS AND METHODS

Cell culture and drug treatment

The glioma cell lines, U251, T98, U87, U373, U118 and A172, were obtained from the American Type Culture Collection (ATCC, Manassas, VA) and cultured according to ATCC protocols.

Enzastaurin was kindly provided by Eli-Lilly. Enzastaurin, Lithium chloride and Kenpaullone (Sigma, St. Louis, MO) were dissolved in 100% DMSO and utilized at the concentrations specified in the manuscript. The GSK3 inhibitor, LY2064827, was kindly provided by Eli-Lilly whereas the GSK3 inhibitors 705701, 708244 and 709125 were kindly provided by The Developmental Therapeutics Program, The National Cancer Institute (Bethesda, MD). Recombinant human TRAIL was from R&D Systems (McKinley Place, MN).

Proliferation assays

Cell proliferation assays were performed by cell counting using Trypan Blue staining for dead cell visualization. Alternatively, a fluorescent assay based on Alamar Blue (BioSource, Camarillo, CA) reduction by viable cells was performed according to the manufacturer's manual.

Gene silencing by siRNA treatment and by generation of stable shRNA cell lines

siRNA duplexes were synthesized by Dharmacon (Chicago, IL): GSK3α (M-003009−01); GSK3β (M-003010−03); NF-κB p65 (cat# MQ-003533−01); c-MYC (cat# L-003282−00). Oligofectamine (Invitrogen, Carlsbad, CA) was utilized for transfection of siRNA into cells per the manufacturer's instructions. shRNA clone for c-MYC V2HS_152050 was from Open Biosytems (Huntsville, AL). Cells stably overexpressing pcDNA6 (Invitrogen) and TMP-MYC-shRNA were selected with 5 μg/ml blasticidin, 1 μg/ml puromycin.

Cell Cycle Analysis

U251 cells were plated at a density of 750,000 in 15 cm tissue culture dishes 24 hours before treatment with enzastuarin started. After 2 hour pulse with 10 mM BrdU (BD Biosciences Pharmingen, San Diego, CA) BrdU-labeled cells were detected as indicated in the user's manual. FACS analysis was performed using FACS-Vantage SE flow cytometer and Cell Quest Acquisition and Analysis software (BD Biosciences).

RNA expression arrays and analysis

U251 cells were treated in triplicates with 10μM enzastaurin for 4, 10 and 18 hours. Total RNA was isolated using TRIZOL (Invitrogen) and further purified using RNeasy Mini Kit (Qiagen, Valencia, CA). Samples were hybridized to Affymetrix Human Genome U133 Plus 2 GeneChip Arrays (Affymetrix, Santa Clara, CA) according to the Affymetrix GeneChip Expression Analysis Technical Manual. The initial gene expression analysis data files (CEL files) were generated using Affymetrix GeneChip Operating Software (GCOS) version 1.2. CEL files were processed as described earlier (11). The false discovery rate of 0.05 and 1.5-fold change were applied as thresholds to select up- or down- regulated probes. Data were analyzed by Ingenuity pathway software analysis. Accession number of the files submitted to NCBI GEO is GSE11285. The sample sets used in figure 8 were previously published in (11, 12).

Real-Time RT-PCR

mRNA expression levels were quantified in triplicates by real-time RT-PCR on an ABI Prism 7900 sequence detection system (Applied Biosystems, Foster City, CA). The relative amount of target transcripts quantified by standard curve method was normalized to the amount of human GAPDH or actin transcripts found in the same sample. Primers and probes were purchased from Applied Biosystems.

Protein analysis by Western Blot, ELISA and Immunohistochemistry

Whole cell lysates were prepared in Cell Lysis Buffer (Cell Signaling Technology Inc., Bevely, MA). Cell lysate samples were run on a pre-cast 4−12% Bis-Tris gel (Invitrogen), transferred to a PVDF membrane (Invitrogen) and probed with the following antibodies: anti-phospho S21/S9 GSK3α/β, (1:2000; Cell Signaling), anti-phGKS3β^{Ser9} and anti-phGSK3β^{Y216} (1/1000; BD Biosciences) anti-β-catenin and anti-phospho-β-catenin^{Ser33,Ser37,Thr41}, anti-phospho c-MYC, T58 (1:1000; Cell Signaling), anti-c-IAP1, anti-c-IAP2 and anti-TRAIL (1/1000; BD Biosciences), anti-GAPDH, anti-c-MYC, N262, NF-κB (1/500) (Santa Cruz Biotechnology, Palo Alto, CA), anti-NF-κBp65 (1/1000; Cell Signaling)β-actin antibody (1:200, Santa Cruz Biotechnology, Santa Cruz, CA). Anti-DR4 and DR5 antibodies were from Chemicon (Temecula, CA). Anti-glycogen antibody and anti-phosphoS^{62} c-MYC were generous gift from Dr. O. Baba (13, 14) and Dr. R. Sears respectively. HRP-conjugated secondary antibodies to rabbit IgG, mouse IgG (1:5000; Cell Signaling), or goat-IgG were used (1:10000; Jackson Immunology Labs, Bar Harbor, ME). All antibodies were diluted in blocking buffer (5% w/v BSA (Sigma), 10mM Tris-HCl, 100 mM NaCl, 0.1% v/v Tween-20).

All other buffers used during Western blotting were made following Invitrogen's NuPage protocol.

Reporter assays and c-MYC activity assay

To measure NF-κB and TCF activity in glioma cell lines we utilized a NF-κB/luciferase reporter plasmid (Stratagene, La Jolla, CA) and pTOPflash reporter plasmid (Upstate, Luzern, Switzerland), respectively. To normalize transfection efficiency, a CMV-βgal plasmid was co-transfected. Reporter activity was detected 24 hours after transfection with the luciferase assay system (Promega Corp., Madison, WI) or β-galactosidase assay system (Promega) on a 20/20n Luminometer (Turner Biosystems, Sunnyvale, CA). c-MYC activity assays were performed with ELISA-based c-MYC activity assay kit (Active Motif, Carlsbad CA) according to the manufacturer's instructions.

GSK3 and Hexokinase in vitro kinase assays

GSK3α and GSK3β kinase activities were measured with the Kinase Profiler Assay Protocol by Upstate (Temecula, CA). Hexokinase activity assays were performed as described elsewhere (15).

In vitro tumorigenicity assays

Colony formation assays were performed using the In vitro tumorigenicity Assay kit from Clontech (Mountain View, CA) according to the manufacturer's instructions. One thousand cells were plated in the upper agar layer per well of 12-well plates. Three or four weeks later colonies were stained and counted.

Tumor Xenograft Models

U87 cells were injected intracranially in neonatal SCID mice or 6−8 week old athymic nude mice (NCI-Frederick Animal Production Area -APA- MD). Stereotaxic coordinates, for injection in adult animals, were 2.8 mm distal to the midline, 1 mm anterior to the coronal suture and 2.5 mm deep from the dura. All procedures were in accordance with NIH Animal Care and Use Committee protocols. Fifteen days after tumor cells injection, enzastaurin (75 mg/kg) and/or carboplatin (40 mg/kg) were administered. Control animals were treated with vehicle alone. For evaluation of tumorigenicity animals were observed daily for death or signs of distress. Kaplan-Meier analysis was performed using Prizm 4 (GraphPad Software Inc., San Diego, CA) or JMP 5.1 (SAS Institute, Cary, NC). Subcutaneous tumor models were generated by injection of 500,000 siRNA-treated U251 cells subcutaneously on the right thigh of 6−8 week old athymic male nude mice. Tumors were measured twice a week.

RESULTS

Inhibition of GSK3 activity results in glioma cell death and reduced tumorigenicity

After we found that enzastaurin exerts direct anti-proliferative and apoptotic effects *in vitro* on multiple glioma cell lines (U87, T98, U251, 373) as well as on primary glioma tumor stem cell (TSC)-like lines (TSC0308 and TSC1228) at therapeutically achievable concentrations (Fig. 1A, 2D, S11 and data not shown), we addressed the mechanism of enzastaurin-induced cytotoxicity through analysis of global gene expression changes over time. Unexpectedly, we found that enzastaurin abnormally regulated expression of a number of WNT pathway genes; Axin 2 showing the most significant change with about 100-fold induction (Table S1, Fig.S1E Other affected genes and pathways, as detected by Anova and Ingenuity Pathway Analysis software, are shown in Tables S2 and S3 respectively). We confirmed activation of the WNT pathway through the demonstration of enzastaurin-mediated loss of β-catenin S37/41 phosphorylation with resultant β-catenin accumulation in the cytoplasm and subsequent

translocation to the nucleus (Fig. S1 A-C). This resulted in a dose-dependent increase in the transcriptional activity of β-catenin (Fig. S1, D and E).

Since GSK3 is known to be a major regulator of β-catenin S37/41 phosphorylation, we asked whether enzastaurin modulates GSK3 activity. We found that the activation-related phosphorylation of Y216/Y276 in GSK3α/β was dramatically decreased following exposure to enzastaurin (Fig. 1B), while inhibitory phosphorylation of GSK3α S21 was significantly up-regulated. Furthermore, the enzymatic activity of both forms of GSK3 was directly down-regulated by 0.5 μM enzastaurin (lowest concentration tested) to less than 3% of the activity of the wild type control enzyme as demonstrated by direct *in vitro* activity assays (Fig. S2).

We next evaluated whether inhibition of GSK3 by other GSK3 inhibitors resulted in glioma cell cytotoxicity. Along with the relatively non-selective GSK3 inhibitors, lithium chloride (LiCl) (16, [17]) and kenpaullone (18) (Fig. S3A-B), we also evaluated several highly selective small molecule GSK3 inhibitors (705701, 708244, 709125 and LY2064827). Serum-cultured U251, U87 and T98 cell lines and two glioma tumor stem cell (TSC)-like lines (11) were analyzed following treatment with each GSK3 inhibitor (Fig S3C). Each drug exerted cytotoxic effects on glioma cell lines in a dose- and time-dependent manner; the most potent of which, LY2064827, demonstrated significant cytotoxicity at concentrations as low as 0.1 μM (Fig S3C). Moreover, the potency of each drug's cytotoxic effects correlated directly with level of decreased phosphorylation of GSK3α/β Y276/Y216 and with increased phosphorylation of GSK3α S21 (Fig. 1B). These results suggest that the cytotoxic effects of these drugs are directly related to their ability to inhibit GSK3 activity.

Direct GSK3 down-regulation inhibits glioma cell proliferation both in vitro and in vivo

To further address the “on-target” specificity of the cytotoxic effects of the GSK3 inhibitors, we examined whether direct down-regulation of GSK3 protein expression inhibits glioma cell growth. GSK3 siRNA-mediated down-regulation of GSK3 resulted in decreased U251 and T98 glioma cell growth (Fig. 1C and data not shown). Furthermore, we observed a 70% reduction in U251 glioma cell clonogenicity as revealed by colony formation assay in soft agar (Fig. 1C). Moreover, there was significant growth delay from GSK3 siRNA treated gliomas *in vivo* compared to siRNA-control treated cells (Fig. 1D). Down-regulation of GSK3 activity by shRNA also resulted in decreased tumor growth in another mouse xenograft model (Fig. S12).

GSK3 down-regulation inhibits anti-apoptotic mechanisms in mitochondria

Since GSK3 is involved in cellular energy metabolism, we investigated the effects of GSK3 inhibition on several parameters of glioma cell glucose metabolism. GSK3 siRNA and enzastaurin significantly inhibited the phosphorylation of the S640 residue of glycogen synthase (GYS), thereby releasing the normal inhibitory effects of GSK3 on GYS (Fig. 2A and S4A) and resulting in increased intracytoplasmic glycogen storage and decreased cytoplasmic glucose concentrations (Fig. 2B).

Majewski *et al.* (15) have demonstrated that a drop in intracellular glucose levels negatively affects the association of Hexokinase (HK) activity with mitochondria, resulting in cellular apoptosis. We, therefore, evaluated the effects of GSK3 inhibition on mitochondrial HK activity. Mitochondrial HK activity decreased by two-fold following GSK3 siRNA or a 4 hour exposure to 5 μM enzastaurin (Fig. S4B-C). By contrast, total and mitochondrial-associated Bax expression significantly increased in the cells treated with GSK3 siRNA or enzastaurin (Fig.2C and S4D), resulting in an increase in the mitochondrial-associated Bax/HKII ratio. (Fig. 2D). Displacement of HKll activity from mitochondria along with increased mitochondrial-associated Bax protein has been shown to lead to a loss of mitochondrial

membrane integrity with resultant apoptosis (19, 20). Indeed, mitochondrial Cytochrome C release was detected and MitoTracker® staining revealed a significant loss of functional mitochondria in enzastaurin, 705701, LY2064827 and GSK3-siRNA treated glioma cells consistent with mitochondrial-mediated cell death (Fig. 2D, and data not shown). The importance of mitochondrial HKll activity in glioma cell survival is supported by the observation that HKll-siRNA mediated down-regulation of HKll induced glioma cell death (Fig. S4E).

GSK3 down-regulation inhibits NF-κB activity essential for glioma cell survival

We and others have previously demonstrated the importance of pro-survival activities of NF-κB in glioma (21-25). Recent studies have linked inhibition of GSK3β to negative regulation of NF-κB activity (6). We found that NF-κB was inhibited by LiCl, kenpaullone, enzastaurin as well as by GSK3 si RNA treatments in U251T98 and U87 (Fig. 3A-B and data not shown). GSK3 inhibition was accompanied by down-regulation of a number of NF-κB regulated pro-survival genes including IL8, IER3, and BIRC2 as assessed by microarray gene expression analysis and TaqMan RT-PCR (Fig. S5A-C). Moreover, NF-κB inhibition resulted in decreased glioma cell survival *in vitro* and in inhibition of tumor growth *in vivo* (Fig. 3C and Fig. 1C). Finally, we also show that up-regulation of NF-κB activity by stable overexpression of NF-κB (p65) results in a partial protection of U251 against GSK3 inhibition-induced cell death (Fig. S9). Thus, GSK3 inhibition contributes to glioma cell death through negative regulation of a number of NF-κB associated pro-survival genes.

GSK3 inhibition increases c-MYC activity and DR4/5 expression in glioma cells

Western blot analysis demonstrated that DR4 (TNFRSF10A), DR5 (TNFRSF10B) proteins and TRAIL were significantly induced by GSK3 inhibition in a time- and a dose-dependent manner (Fig. 4A-C and data not shown). Since c-MYC activity is partially regulated by GSK3, and since c-MYC is known to regulate the transcription of DR5 (26, 27), we evaluated c-MYC activity following GSK3 inhibition. An ELISA-based DNA-binding assay demonstrated that c-MYC activity was up-regulated after 4 hours of enzastaurin treatment and by GSK3 siRNA (Fig. 5A).

The stability and thus activity of c-MYC is specifically regulated by differential phosphorylation of its N-terminus through GSK3-mediated inhibitory phosphorylation of c-MYC T58 and through ERK1/2 activating phosphorylation of c-MYC S62 (28-30). We found that both enzastaurin and GSK3 siRNA induced loss of the inhibitory phosphorylation of c-MYC at T58 and increased phosphorylation of the activating phosphorylation site S62 (Fig. 5B, S10 and data not shown). Consistent with increased c-MYC S62 phosphorylation, treatment with different GSK3 inhibitors induced ERK1/2 phopshorylation (Fig. S6). ERK1/2 activation was sustained (Fig. S6A) and dose-dependent (Fig. S6B) suggesting that ERK1/2 might be responsible for the phosphorylation of c-MYC S62 in glioma cells as has been reported previously for other cell types (28).

We next examined whether c-MYC regulates transcription of Bax and TRAIL-associated death receptors in glioma cell lines, as has been demonstrated in other cells (for a review see (31)). Treatment of glioma cells with c-MYC siRNA resulted in significant down-regulation of Bax, DR4 and DR5 both at the RNA (Fig. S7A-C) and protein levels (Fig. 5C). Moreover, down-regulation of c-MYC expression, by stable transfection of a c-MYC shRNA in U251, resulted in almost complete protection against GSK3 inhibitors cytotoxicity (Fig. 5D). Consistent with the cytotoxicity assays, 40% of parental U251 cell mitochondria completely lost their transmembrane potential 24 hours after exposure to 705701, whereas an insignificant percentage of cells lost their mitochondria transmembrane potential in the c-MYC shRNA-stably transfected glioma cells exposed to 705701 (Fig. S7H). By contrast, c-MYC

overexpression was cytotoxic to glioma cells (Fig. 6B) and positively regulated transcription of Bax, DR4 and DR5 (Fig. S7D-F).

Finally, we demonstrate that GSK3 inhibition resulted in significantly increased levels of both Bim RNA and protein, a known Bcl-2 antagonist and c-MYC target gene (Fig. S7I-J and data not shown) (32). These observations are consistent with the hypothesis that c-MYC plays a significant, if not predominant, role as a mediator of GSK3 inhibition-induced glioma cell apoptosis.

GSK3 inhibitors and TRAIL act synergistically in glioma cell cytotoxicity

We found that in addition to DR4/5, TRAIL was up-regulated by enzastaurin treatment and GSK3 siRNA (Fig. 4C) in several glioma cell lines. Given that glioma cells are relatively resistant to TRAIL-induced apoptosis and that GSK3 inhibition up-regulates the death receptors, Bax and TRAIL, and inhibits the anti-apoptotic HKll/mitochondrial and NF-κB mechanisms, we examined whether GSK3 inhibition would result in increased sensitivity to apoptotic stimuli such as TRAIL itself. We found that TRAIL-mediated cell death was dramatically enhanced when otherwise sub-cytotoxic doses of TRAIL (25−50 nM) and enzastaurin (1 − 2.5 μM) were combined in U251 (Fig. 6A) and U87 (data not shown) cell lines. Similar data were obtained with other GSK3 inhibitors 705701 (0.05−0.1μM) and LY2064827(0.05 μM) as well as with GSK3 siRNA (data not shown). Moreover, overexpression of c-MYC rendered cells more sensitive to TRAIL-mediated cytotoxicity (Fig. 6B), again supporting the hypothesis of the important role of c-MYC in GSK3-induced cytotoxicity. Finally, enzastaurin combined with carboplatin, a standard DNA damaging chemotherapeutic agent often used in patients with malignant gliomas, causes synergistic tumor killing both *in vitro* and *in vivo* (Fig. 6C and D) confirming our hypothesis that GSK3 inhibition would have additive/synergistic cytotoxic activity in combination with other, unrelated DNA damaging agents.

DISCUSSION

Although initially viewed as a specific regulator of glycogen metabolism, GSK3 has recently been shown to be a crucial enzymatic regulator of a diverse number of cellular functions including cell structure, metabolism, and survival (reviewed in (4, 5)). Our work demonstrates a role for GSK3 inhibition in mediating glioma cell proliferation arrest, decreased clonogenicity and induction of apoptotic cell death through both the extrinsic and intrinsic apoptotic pathways both *in vitro* and *in vivo*, much of which is mediated through c-MYC.

c-MYC is known to play important roles in the regulation of cell proliferation, differentiation and apoptosis and is deregulated in many human tumors (33, 34), including glioma (35-37) (Fig. S8). c-MYC can be activated by phosphorylation at S62 by MAP kinase ERK1/2 (extracellular signal-related protein kinase2) whereas it is inhibited by GSK3-mediated phosphorylation at T58 (28). We show that the increase in c-MYC activity in glioma cells after GSK3 inhibition correlates with a loss of T58 phosphorylation and with an increase in S62 phosphorylation. The decrease in c-MYC phosphorylation at T58 observed following enzastaurin or GSK3 siRNA treatment correlates with the inhibition of Tyrosine 216/276 phosphorylation of GSK3α/GSK3β and is therefore likely to be a direct result of decreased GSK3 activity. By contrast the increase in c-MYC S62 phosphorylation coincides with an increase in activating ERK1/2 phosphorylation consistent with the recent demonstration that GSK3 negatively regulates ERK1/2 activity (38). Thus, inhibition of GSK3 activity results in increased phosphorylation and activity of ERK1/2, as we demonstrated in figure S6. In addition to a likely direct effect of ERK1/2 on activation of c-MYC, sustained phosphorylation of ERK1/2 and its target p90rSK have been shown to induce cell cycle arrest (39), as we observed in our enzastaurin and GSK3 siRNA treated cells (Fig. S6 and data not shown). Seth and co-

workers have suggested that the elevated Cdk1/CyclinB levels seen in G2/M may mediate the increased S62 phosphorylation of c-MYC observed in G2/M (40). This is consistent with our data demonstrating up-regulation of Cyclin B following enzastaurin and GSK3 siRNA induced G2/M arrest prior to induction of apoptosis (data not shown). Whether GSK3-inhibition-induced phosphorylation of c-MYC S62 is mediated directly by ERK1/2 and/or G2/M arrested cellular up-regulation of Cdk1/cyclin B remains a subject of future studies.

GSK3 inhibition-mediated up-regulation of c-MYC activity results in increased expression of apoptosis-related molecules DR5, Bim, Bax and TRAIL and down-regulation of anti-apoptotic protein, FLIP (data not shown), all known targets of c-MYC (27, 31). DR4 may also be a target of c-MYC transcriptional activity in glioma cells since siRNA-mediated down-regulation of c-MYC resulted in decreased mRNA and protein levels of DR4 whereas overexpression of c-MYC up-regulates DR4 (Fig. S7). Our demonstration that reduction of c-MYC activity by shRNA protects glioma cells from GSK3-mediated cytotoxicity, together with data reported by Rottman and co-workers, suggests that c-MYC plays a major role as a mediator of GSK3 inhibition-related induction of TRAIL-mediated apoptosis (41).

In addition to induction of apoptosis through a TRAIL-mediated mechanism, our data also demonstrates that GSK3 inhibition may increase the propensity for glioma cell death through direct destabilization of the mitochondrial membrane. HK can inhibit apoptosis-related mitochondrial Cytochrome C release by interfering with the ability of Bax to bind to the outer mitochondrial membrane (19). We show that treatment of glioma cells with GSK3 inhibitors results in increased mitochondria - associated Bax protein, accompanied by a decrease in mitochondria - associated HKII activity (Fig. 2 and S4). Increases in the Bax/HKll ratio on the outer mitochondrial membrane have been previously demonstrated to result in loss of mitochondrial membrane potential with subsequent mitochondrial Cytochrome C release and apoptosis, as we observed following GSK3 inhibition in glioma cells.

Although the exact mechanism for HK dissociation from mitochondria following GSK3 inhibition remains the subject of future experiments, it has been previously demonstrated that reduction in intracellular glucose content induces dissociation of HK from mitochondria (15). Thus, it is likely that the nearly two-fold reduction in intracellular glucose concentration we observed in glioma cells following GSK3 inhibition is at least partially responsible for the HK dissociation from mitochondria. The reduction in intracellular glucose content following GSK3 inhibition is likely a result of decreased GSK3-dependent inhibitory GYS S640 phosphorylation resulting in over-stimulation of GYS activity and leading to the increased intracellular glycogen content we observed.

Finally, we demonstrated that down-regulation of GSK3 activity led to a decrease in NF-κB activity within glioma cells; an important finding since down-regulation of NF-κB by siRNA or by pharmacological means (salicylates, velcade) results in increased propensity for glioma cell death ((23) and unpublished data). These observations are in agreement with those from other groups who have demonstrated regulation of MEF and pancreatic cancer cell survival by GSK3β through an NF-κB-dependent pathway (6). Whether the effect of GSK3 inhibition on NF-κB activity in glioma cells is mediated by direct phosphorylation of NF-κB components as previously described (9, 42), or through the upstream regulators, IKK and IKB (43), and/or through inhibitory binding by increased nuclear β-catenin (44, 45) remains a matter of further study.

It is interesting to note that a significant number of GBMs (as well as many other cancer types) have mutations/deletions of the PTEN gene locus leading to constitutive AKT activation. This likely results in constitutive down-regulation of GSK3 activity through S9 phosphorylation by AKT (46). This constitutive inhibition of GSK3 activity may in part be responsible for the up-

regulation c-MYC activity in gliomas (Figure S8) and a number of other tumors that do not have amplification of the c-MYC gene (35-37). The higher basal level of c-MYC activity found in glioma and tumor cells may subsequently make them significantly more sensitive to c-MYC-induced apoptosis following application of GSK3 inhibitors compared to normal cells that start out with low levels of c-MYC activity. Thus, it is plausible that deregulation of the PI3K pathway and activation of AKT may be a synthetic lethal event for further GSK3 inhibition. If so, patients suffering from tumors with constitutive active AKT may ultimately prove to be preferentially sensitive to therapeutic GSK3 inhibition. Additional *in vitro* and *in vivo* experimental data will clearly be needed to test this hypothesis.

In conclusion, we have demonstrated that GSK3 inhibition in glioma cells leads to; i, induction of pro-apoptotic effects through priming of the TRAIL death receptor pathway (GSK3/c-MYC/DR4/DR5/TRAIL/Bim); ii, inhibition of pro-survival signals through inhibiting NF-κB activity; iii, induction of mitochondrial permeability (Bax/HKll ratio) through alteration intracellular glucose regulation (GSK3/GYS). These data suggest that GSK3 may be an important molecular target for human glioma therapy. Future studies will need to better define the optimal combinations of GSK3 inhibitors and cytotoxic agents in additional models of glioma and other cancers in order to better understand and optimize the most promising therapeutic strategies to evaluate in the clinic.

ACKNOWLEGEMENTS

We acknowledge The Developmental Therapeutics Program, The National Cancer Institute (Bethesda, MD) and Dr. Zaharevitz for kindly provided GSK3 inhibitors 705701, 708244 and 709125. We are thankful to Dr. Sears for providing us with an aliquot of anti-phospho S62 c-MYC antibody, to Dr. Baba for a generous gift of the anti-glycogen-specific antibody, and to Dr. Nogueira for sharing her detailed protocol with us on Hexokinase activity assays (NF-κB plasmid was kindly provided by Drs. Bren and Paya from Mayo Clinic College of Medicine). We also thank Mr. James W. Nagle and Ms. Deborah Kauffman from NINDS sequencing facility and Dr. Carolyn L. Smith from NINDS light image facility for their valuable contributions to this work. This research was supported by the Intramural Research Program of the NIH, National Cancer Institute, Center for Cancer Research.

REFERENCE LIST

1. Graff JR, McNulty AM, Hanna KR, et al. The protein kinase Cbetaselective inhibitor, Enzastaurin (LY317615.HCl), suppresses signaling through the AKT pathway, induces apoptosis, and suppresses growth of human colon cancer and glioblastoma xenografts. Cancer Res Aug 15;2005 65(16):7462–9. [PubMed: 16103100]
2. Fine, HA.; Royce, C.; Draper, D.; Haggarty, I., et al. Results from phase II trial of enzastaurin (LY317615) in patients with recurrent high grade gliomas.. Journal of Clinical Oncology, 2005 ASCO Annual Meeting Proceedings; 2005: American Society of Clinical Oncology; 2005; p. 1504
3. Embi N, Rylatt DB, Cohen P. Glycogen synthase kinase-3 from rabbit skeletal muscle. Separation from cyclic-AMP-dependent protein kinase and phosphorylase kinase. Eur J Biochem Jun;1980 107 (2):519–27. [PubMed: 6249596]
4. Cohen P, Goedert M. GSK3 inhibitors: development and therapeutic potential. Nat Rev Drug Discov Jun;2004 3(6):479–87. [PubMed: 15173837]
5. Jope RS, Johnson GV. The glamour and gloom of glycogen synthase kinase-3. Trends Biochem Sci Feb;2004 29(2):95–102. [PubMed: 15102436]
6. Hoeflich KP, Luo J, Rubie EA, Tsao MS, Jin O, Woodgett JR. Requirement for glycogen synthase kinase-3beta in cell survival and NF-kappaB activation. Nature Jul 6;2000 406(6791):86–90. [PubMed: 10894547]
7. Pap M, Cooper GM. Role of glycogen synthase kinase-3 in the phosphatidylinositol 3-Kinase/Akt cell survival pathway. J Biol Chem Aug 7;1998 273(32):19929–32. [PubMed: 9685326]
8. Ougolkov AV, Fernandez-Zapico ME, Savoy DN, Urrutia RA, Billadeau DD. Glycogen synthase kinase-3beta participates in nuclear factor kappaB-mediated gene transcription and cell survival in pancreatic cancer cells. Cancer Res Mar 15;2005 65(6):2076–81. [PubMed: 15781615]

9. Demarchi F, Bertoli C, Sandy P, Schneider C. Glycogen synthase kinase-3 beta regulates NF-kappa B1/p105 stability. J Biol Chem Oct 10;2003 278(41):39583–90. [PubMed: 12871932]
10. Tan J, Zhuang L, Leong HS, Iyer NG, Liu ET, Yu Q. Pharmacologic modulation of glycogen synthase kinase-3beta promotes p53-dependent apoptosis through a direct Bax-mediated mitochondrial pathway in colorectal cancer cells. Cancer Res Oct 1;2005 65(19):9012–20. [PubMed: 16204075]
11. Lee J, Kotliarova S, Kotliarov Y, et al. Tumor stem cells derived from glioblastomas cultured in bFGF and EGF more closely mirror the phenotype and genotype of primary tumors than do serum-cultured cell lines. Cancer Cell May;2006 9(5):391–403. [PubMed: 16697959]
12. Sun L, Hui AM, Su Q, et al. Neuronal and glioma-derived stem cell factor induces angiogenesis within the brain. Cancer Cell Apr;2006 9(4):287–300. [PubMed: 16616334]
13. MacAulay K, Blair AS, Hajduch E, et al. Constitutive activation of GSK3 down-regulates glycogen synthase abundance and glycogen deposition in rat skeletal muscle cells. J Biol Chem Mar 11;2005 280(10):9509–18. [PubMed: 15632169]
14. Baba O. [Production of monoclonal antibody that recognizes glycogen and its application for immunohistochemistry]. Kokubyo Gakkai Zasshi Jun;1993 60(2):264–87. [PubMed: 8345245]
15. Majewski N, Nogueira V, Robey RB, Hay N. Akt inhibits apoptosis downstream of BID cleavage via a glucose-dependent mechanism involving mitochondrial hexokinases. Mol Cell Biol Jan;2004 24(2):730–40. [PubMed: 14701745]
16. Klein PS, Melton DA. A molecular mechanism for the effect of lithium on development. Proc Natl Acad Sci U S A Aug 6;1996 93(16):8455–9. [PubMed: 8710892]
17. Davies SP, Reddy H, Caivano M, Cohen P. Specificity and mechanism of action of some commonly used protein kinase inhibitors. Biochem J Oct 1;2000 351(Pt 1):95–105. [PubMed: 10998351]
18. Cole A, Frame S, Cohen P. Further evidence that the tyrosine phosphorylation of glycogen synthase kinase-3 (GSK3) in mammalian cells is an autophosphorylation event. Biochem J Jan 1;2004 377(Pt 1):249–55. [PubMed: 14570592]
19. Pastorino JG, Hoek JB. Hexokinase II: the integration of energy metabolism and control of apoptosis. Curr Med Chem Aug;2003 10(16):1535–51. [PubMed: 12871125]
20. Robey RB, Hay N. Mitochondrial hexokinases, novel mediators of the antiapoptotic effects of growth factors and Akt. Oncogene Aug 7;2006 25(34):4683–96. [PubMed: 16892082]
21. Kasuga C, Ebata T, Kayagaki N, et al. Sensitization of human glioblastomas to tumor necrosis factor-related apoptosis-inducing ligand (TRAIL) by NF-kappaB inhibitors. Cancer Sci Oct;2004 95(10): 840–4. [PubMed: 15504253]
22. Robe PA, Bentires-Alj M, Bonif M, et al. In vitro and in vivo activity of the nuclear factor-kappaB inhibitor sulfasalazine in human glioblastomas. Clin Cancer Res Aug 15;2004 10(16):5595–603. [PubMed: 15328202]
23. Hui AM, Zhang W, Chen W, et al. Agents with selective estrogen receptor (ER) modulator activity induce apoptosis in vitro and in vivo in ER-negative glioma cells. Cancer Res Dec 15;2004 64(24): 9115–23. [PubMed: 15604281]
24. Samanta AK, Huang HJ, Bast RC Jr. Liao WS. Overexpression of MEKK3 confers resistance to apoptosis through activation of NFkappaB. J Biol Chem Feb 27;2004 279(9):7576–83. [PubMed: 14662759]
25. Tran NL, McDonough WS, Savitch BA, et al. Increased Fibroblast Growth Factor-Inducible 14 Expression Levels Promote Glioma Cell Invasion via Rac1 and Nuclear Factor-{kappa}B and Correlate with Poor Patient Outcome. Cancer Res Oct 1;2006 66(19):9535–42. [PubMed: 17018610]
26. Wang Y, Engels IH, Knee DA, Nasoff M, Deveraux QL, Quon KC. Synthetic lethal targeting of MYC by activation of the DR5 death receptor pathway. Cancer Cell May;2004 5(5):501–12. [PubMed: 15144957]
27. Ricci MS, Jin Z, Dews M, et al. Direct repression of FLIP expression by c-myc is a major determinant of TRAIL sensitivity. Mol Cell Biol Oct;2004 24(19):8541–55. [PubMed: 15367674]
28. Sears R, Nuckolls F, Haura E, Taya Y, Tamai K, Nevins JR. Multiple Ras-dependent phosphorylation pathways regulate Myc protein stability. Genes Dev Oct 1;2000 14(19):2501–14. [PubMed: 11018017]

29. Seth A, Alvarez E, Gupta S, Davis RJ. A phosphorylation site located in the NH2-terminal domain of c-Myc increases transactivation of gene expression. J Biol Chem Dec 15;1991 266(35):23521–4. [PubMed: 1748630]
30. Gupta S, Seth A, Davis RJ. Transactivation of gene expression by Myc is inhibited by mutation at the phosphorylation sites Thr-58 and Ser-62. Proc Natl Acad Sci U S A Apr 15;1993 90(8):3216–20. [PubMed: 8386367]
31. Sheikh MS. Myc tagging along the TRAIL to death receptor 5. Cell Cycle Jul;2004 3(7):920–2. [PubMed: 15254425]
32. Egle A, Harris AW, Bouillet P, Cory S. Bim is a suppressor of Myc-induced mouse B cell leukemia. Proc Natl Acad Sci U S A Apr 20;2004 101(16):6164–9. [PubMed: 15079075]
33. Nesbit CE, Tersak JM, Prochownik EV. MYC oncogenes and human neoplastic disease. Oncogene May 13;1999 18(19):3004–16. [PubMed: 10378696]
34. Oster SK, Ho CS, Soucie EL, Penn LZ. The myc oncogene: MarvelouslY Complex. Adv Cancer Res 2002;84:81–154. [PubMed: 11885563]
35. Collins VP. Gene amplification in human gliomas. Glia Nov;1995 15(3):289–96. [PubMed: 8586464]
36. McDonald JD, Dohrmann GJ. Molecular biology of brain tumors. Neurosurgery Nov;1988 23(5): 537–44. [PubMed: 3059215]
37. Sehgal, Am. Molecular changes during the genesis of human gliomas. Semin Surg Oncol Jan-Feb; 1998 14(1):3–12. [PubMed: 9407626]
38. Wang Q, Zhou Y, Wang X, Evers BM. Glycogen synthase kinase-3 is a negative regulator of extracellular signal-regulated kinase. Oncogene Jan 5;2006 25(1):43–50. [PubMed: 16278684]
39. Goulet AC, Chigbrow M, Frisk P, Nelson MA. Selenomethionine induces sustained ERK phosphorylation leading to cell-cycle arrest in human colon cancer cells. Carcinogenesis Jan;2005 26(1):109–17. [PubMed: 15513932]
40. Seth A, Gupta S, Davis RJ. Cell cycle regulation of the c-Myc transcriptional activation domain. Mol Cell Biol Jul;1993 13(7):4125–36. [PubMed: 8321217]
41. Rottmann S, Wang Y, Nasoff M, Deveraux QL, Quon KC. A TRAIL receptor-dependent synthetic lethal relationship between MYC activation and GSK3beta/FBW7 loss of function. Proc Natl Acad Sci U S A Oct 18;2005 102(42):15195–200. [PubMed: 16210249]
42. Schwabe RF, Brenner DA. Role of glycogen synthase kinase-3 in TNF-alpha-induced NF-kappaB activation and apoptosis in hepatocytes. Am J Physiol Gastrointest Liver Physiol Jul;2002 283 (1):G204–11. [PubMed: 12065308]
43. Takada Y, Fang X, Jamaluddin MS, Boyd DD, Aggarwal BB. Genetic deletion of glycogen synthase kinase-3beta abrogates activation of IkappaBalpha kinase, JNK, Akt, and p44/p42 MAPK but potentiates apoptosis induced by tumor necrosis factor. J Biol Chem Sep 17;2004 279(38):39541–54. [PubMed: 15252041]
44. Deng J, Miller SA, Wang HY, et al. beta-catenin interacts with and inhibits NF-kappa B in human colon and breast cancer. Cancer Cell Oct;2002 2(4):323–34. [PubMed: 12398896]
45. Deng J, Xia W, Miller SA, Wen Y, Wang HY, Hung MC. Crossregulation of NF-kappaB by the APC/GSK-3beta/beta-catenin pathway. Mol Carcinog Mar;2004 39(3):139–46. [PubMed: 14991743]
46. Cross DA, Alessi DR, Cohen P, Andjelkovich M, Hemmings BA. Inhibition of glycogen synthase kinase-3 by insulin mediated by protein kinase B. Nature Dec 21−28;1995 378(6559):785–9. [PubMed: 8524413]

Supplementary Material

Refer to Web version on PubMed Central for supplementary material.

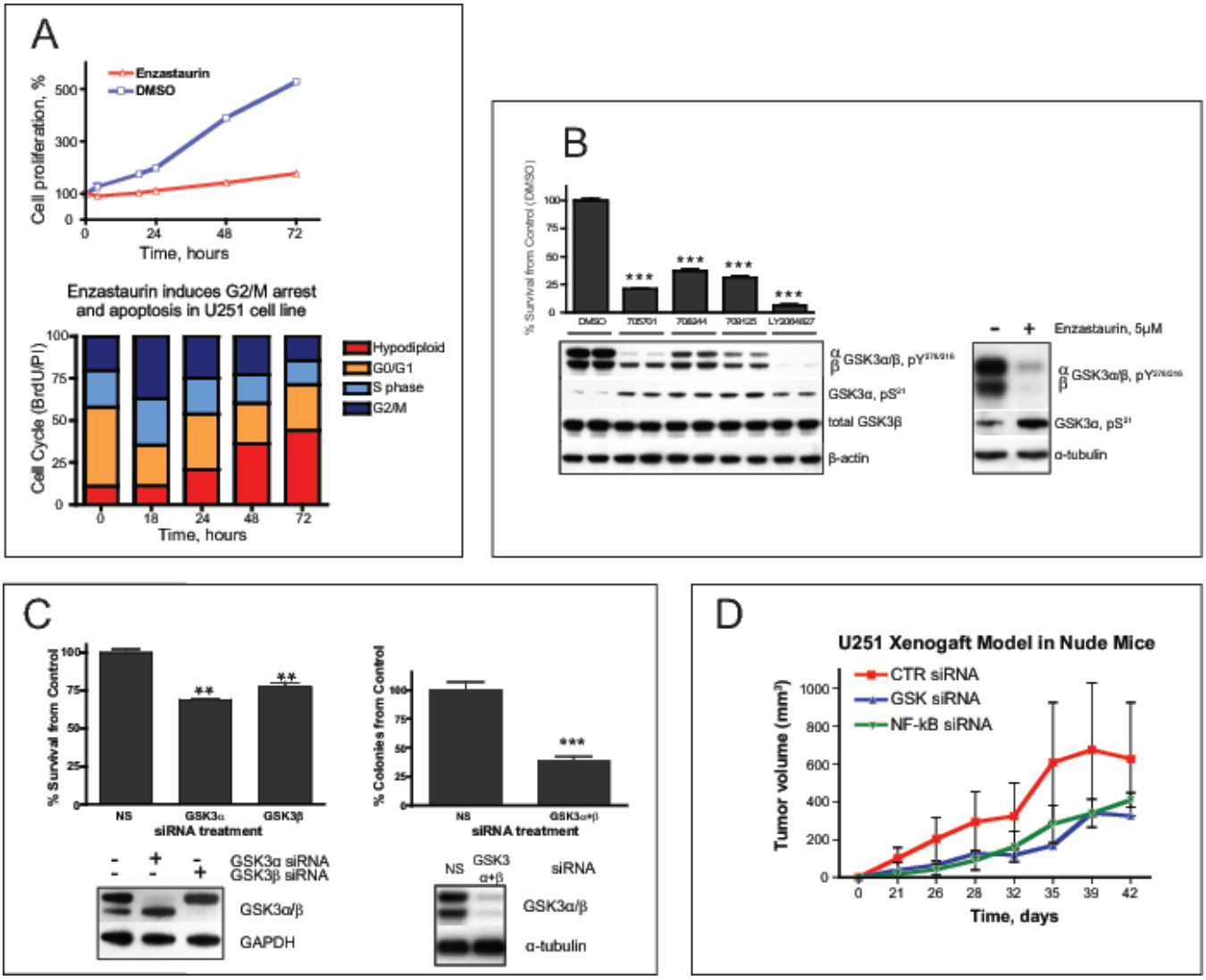

Figure 1. GSK3 inhibitors and siRNA result in glioma cell death and reduced tumorigenicity

(A) Cytotoxicity of enzastaurin (5 μM) in U251 glioma cell line as determined by a cell-counting assay at different time points as indicated. Bar graph shows results of the cell cycle analysis of U251 cells exposed to enzastaurin for the indicated time, then labeled with10 μM BrdU for 2 hours The drug induces G2/M arrest at 18 hours and subsequent apoptosis. **(B)** Changes in phosphorylation of GSK3 at Y276/216 and S21 of GSK3α caused by different GSK3 inhibitors correlate with survival of U251. Cells were treated with 0.5 μM of the indicated drugs for 48 hours Cell survival was assessed by cell counting (upper panel, graph). Y216/279 activating phosphorylation and S21 inhibitory phosphorylation of GSK3α/β were measured by Western Blot (lower panel). Here and below the asterisks designate p-values (t-test) as follows: *, $p<0.05$; ** , $p<0.005$ and ***, $p<0.00$, the error bars represent standard deviation. **(C)** GSK3 siRNA inhibits proliferation of glioma cells *in vitro* and *in vivo* (upper left corner). GSK3-specific siRNAs were transfected into U251 cells. Cells were harvested and counted 48 hours after transfection. Western blot shows efficiency of protein silencing by siRNA. In vitro clonogenicity assay demonstrated reduced number of colonies derived from U251 cells treated with GSK3 siRNA compared to non silencing (NS) siRNA. **(D)** Subcutaneous xenograft model in nude mice. After treatment with control, GSK3, or NF-κB siRNAs, 0.5 million U251 cells were injected subcutaneously into the thighs of nude mice.

Each group consisted of 6 animals. Tumors were measured twice a week. The results are presented as tumor volume.

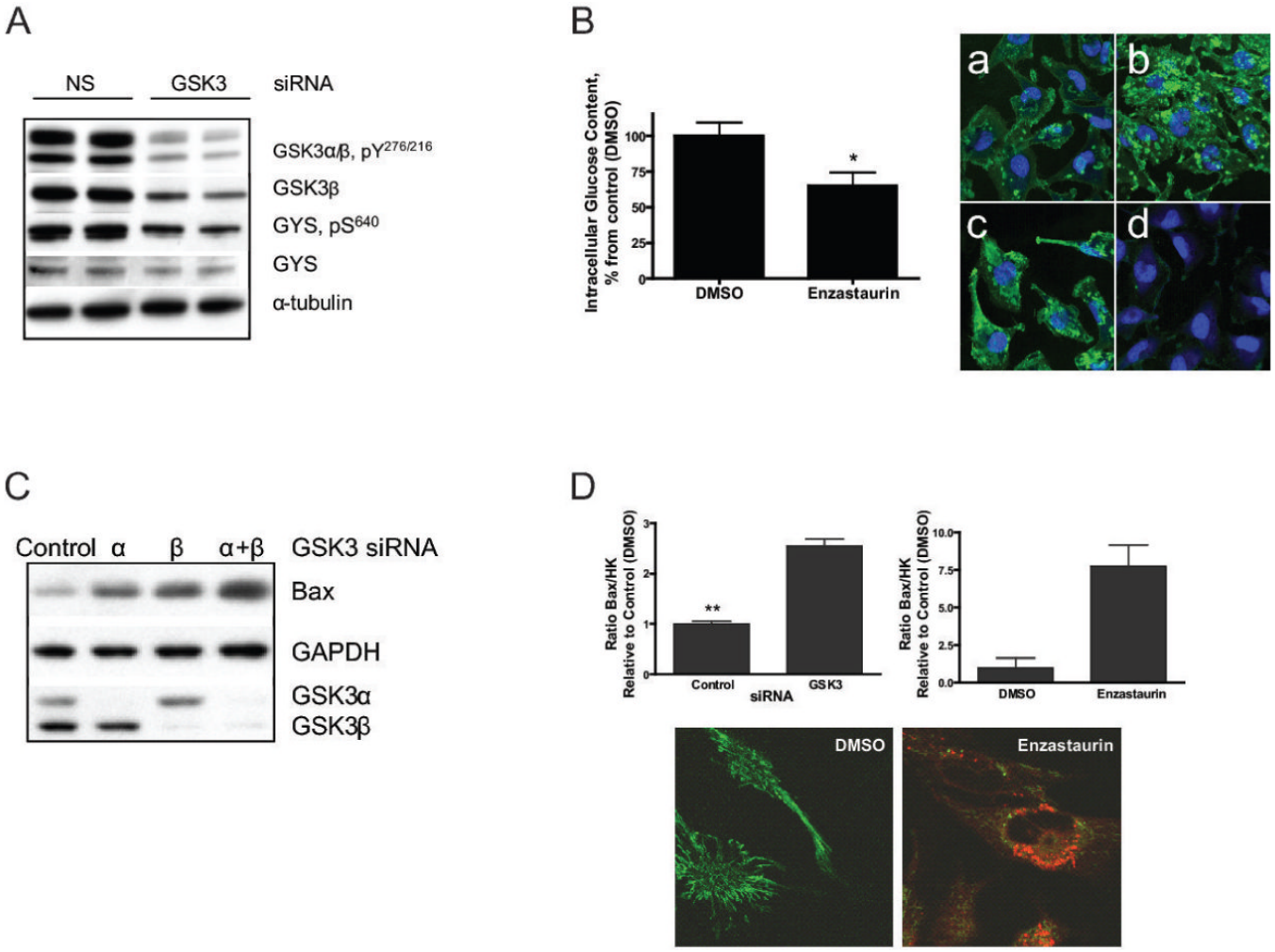

Figure 2. Inhibition of GSK3 activity in glioma cell lines leads to changes in glucose regulation and in anti-apoptotic mechanisms in mitochondria

(A) Western Blot analysis of GSK3 siRNAs treated cell lysates show that GSK3 siRNAs decrease S640 phosphorylation of GYS in U251 (48 hours after transfection). **(B)** Bar graph shows glucose levels decrease in U251 cells treated with enzastaurin, 5 μM for 4 hours. Immunocytochemistry staining with anti-glycogen antibody revealed that GSK3 inhibition resulted in increased glycogen stores in the glioma cells. U251 cells were treated with (a) DMSO (4hours), (b) enzastaurin, 5μM (4hours); (c) insulin (30 minutes); (d) glucoamylase (3 hours) Glucoamylase digests glycogen and therefore is used as a negative control. The similar data were obtained with 705701 and LY2064827. **(C)** Western blot analysis of Bax levels in U251 treated with control or GSK3 siRNA. **(D)** Ratio of Bax/HK activity in mitochondria fractions is increased with GSK3 siRNA (48 hours) and enzastaurin treatments (4 hours). MitoTracker® Green staining of the functional mitochondria in DMSO and 5μM enzastaurin treated living U251 cells. Red color in the right panel shows fluorescence of enzastaurin.

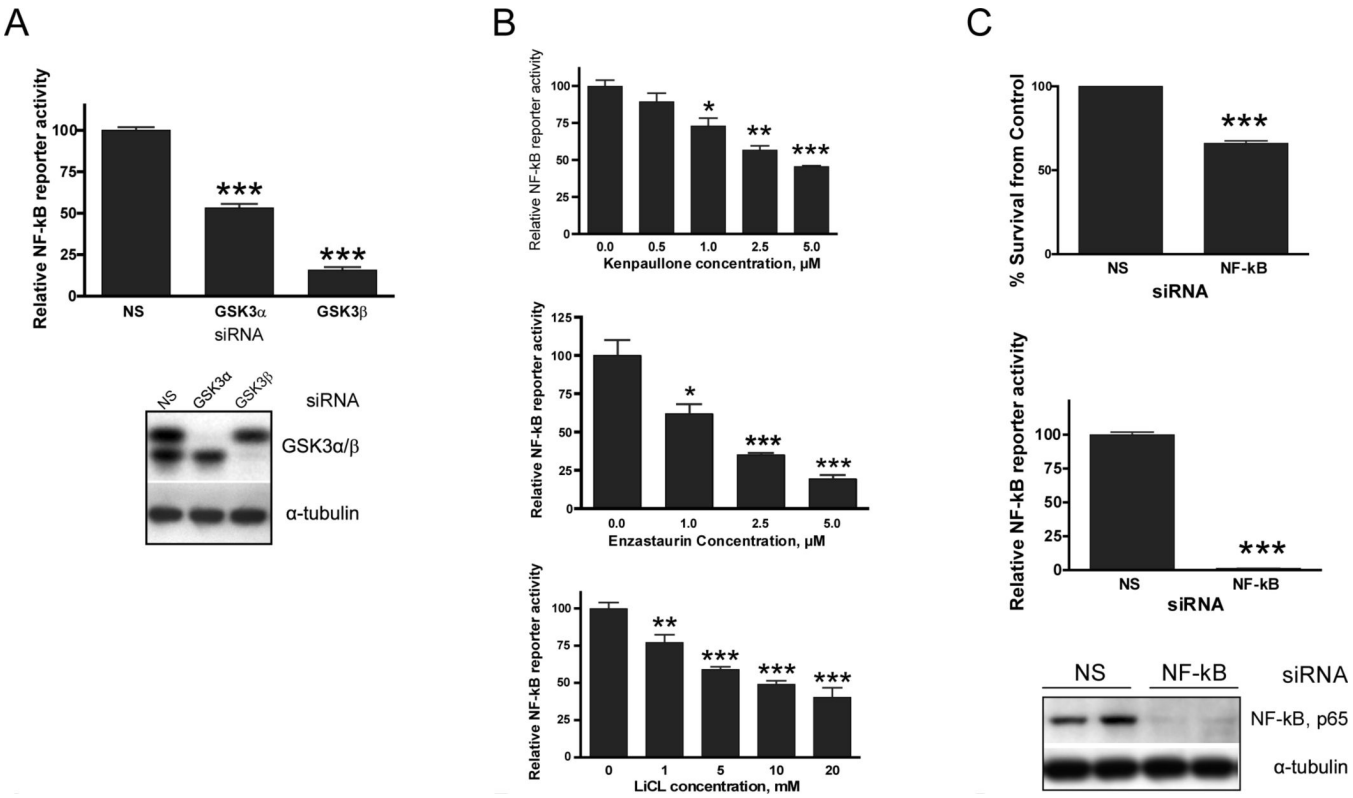

Figure 3. Cytotoxicity caused by GSK3 inhibition is accompanied by down-regulation of NF-κB activity

NF-κB luciferase reporter assay shows that GSK3 siRNA **(A)** down-regulates NF-κB activity in U251. **(B)** Kenpaullone, LiCl and enzastaurin down-regulate NF-κB activity in a dose-dependent manner (24 hours of treatment). **(C)** NF-κB silencing by siRNA resulted in cytotoxicity of U251. Lower graph shows functional efficiency of NF-κB activity silencing by siRNA in U251 as measured by luciferase reporter assay (NS, non-silencing control siRNA). In all luciferase assays cells were cotransfected with luciferase reporters for NF-κB and b-gal. Luciferase activity levels from NF-κB reporter were divided by those from the b-gal reporter. To control for transfection efficiency and cell viability, a CMV-βgal plasmid was co-transfected. NF-κB and β-galactosidase reporter activities were detected 24 hours after transfection and NF-κB values were normalized compared to β-galactosidase levels. Western Blot shows the efficiency of NF-κB silencing by siRNA.

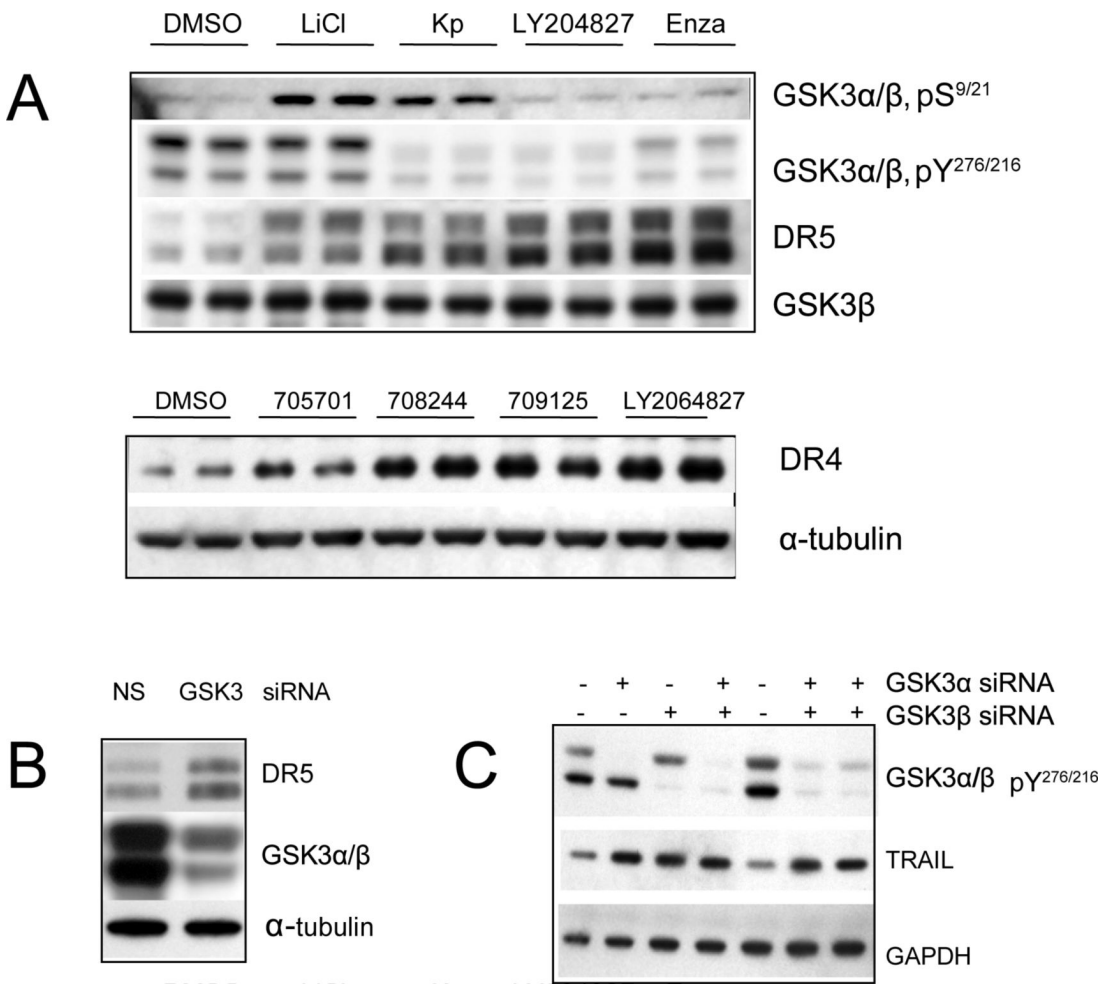

Figure 4. GSK3 inhibition results in up-regulation of Death Receptors and TRAIL

Western blot of total U251 cell lysates shows that DR4 and DR5 are up-regulated with **(A)** GSK3 inhibitors as indicated (all at a 0.5 μM concentration for 24 hours of treatment) **(B)** and by GSK3 siRNAs. **(C)** TRAIL is up-regulated by GSK3siRNA (48 hours of treatment).

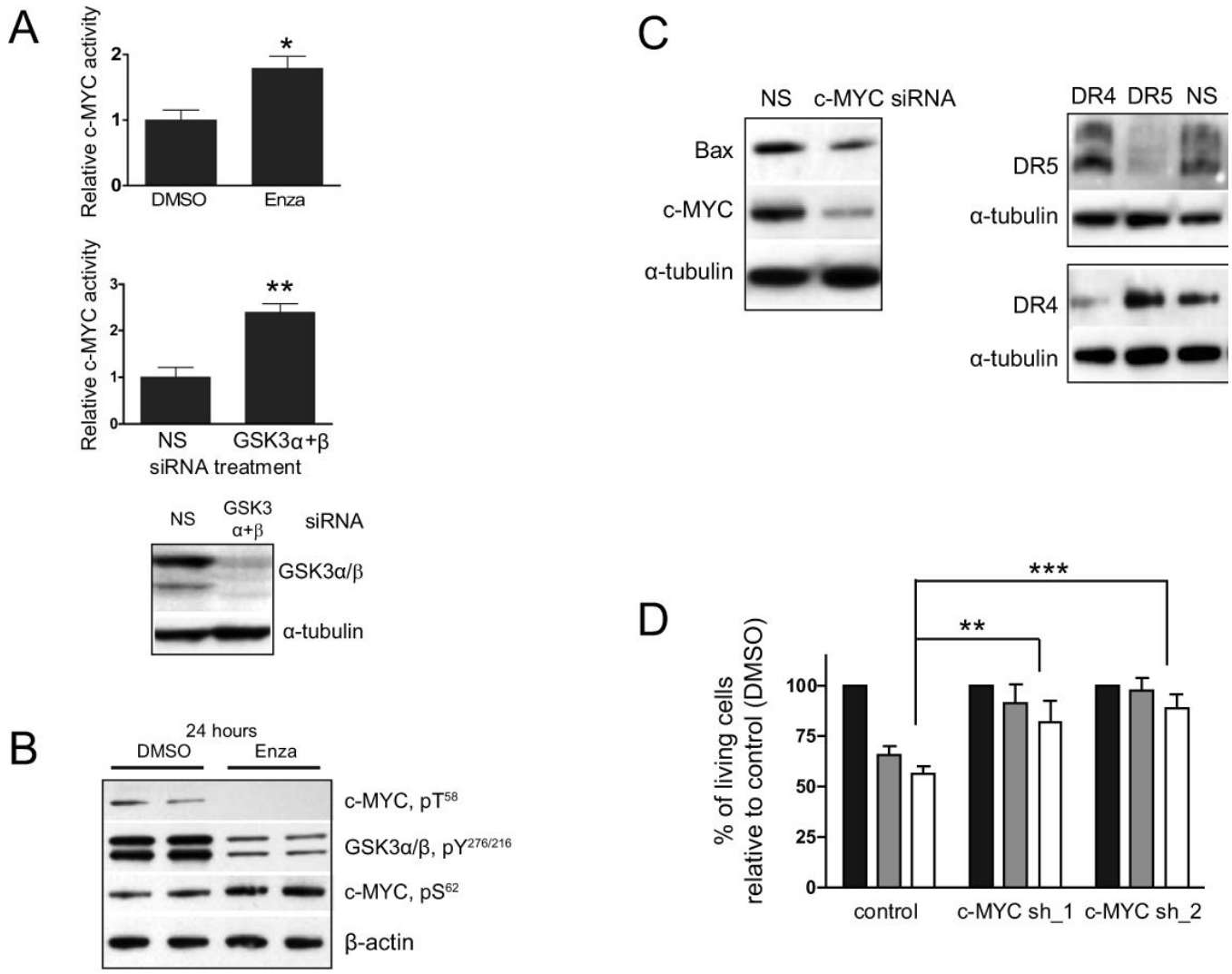

Figure 5. c-MYC is mediator of GSK3 inhibition-mediated cytotoxicity

(A) GSK3 inhibition by siRNA and enzastaurin up-regulates c-MYC activity as revealed by ELISA-based DNA-binding assay **(B)** WB analysis of nuclear extracts prepared from cells treated with 5 μM enzastaurin or DMSO. c-MYC phosphorylation at T58 is down-regulated in U251. This correlates with reduced Y phosphorylation of GSK3, both at 4 and 24 hours (shown) of treatment with enzastaurin. Conversely, S62 phosphorylation of c-MYC was up-regulated at 24 hours **(C)** Western Blot of total cell lysates: c-MYC siRNA negatively regulates Bax, DR4 and DR5 proteins in U251. NS, non-silencing control siRNA. **(D)** Silencing of c-MYC in U251 by shRNA in two individual clones, c-MYC-shRNA_1 & 2, effectively protects cells from 0.5 μM 705701 or from 0.5 μM LY2064827 (24 hours treatment) compared to control cells. Cells were plated at a density of 50,000 per well in a 6-well plate.

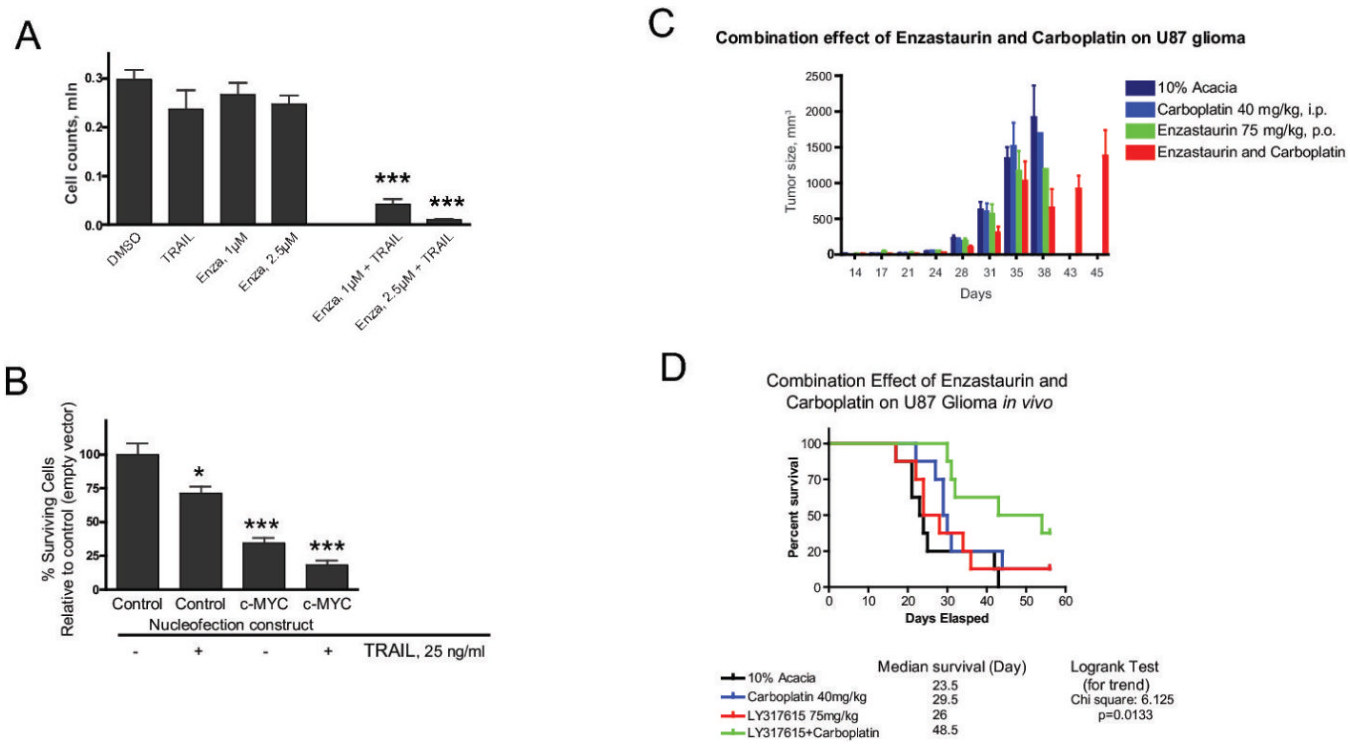

Figure 6. GSK3 inhibition potentiates the anti-tumor action of other cytotoxic drugs *in vitro* and *in vivo*

(A) TRAIL acts synergistically with enzastaurin in glioma cell killing. **(B)** Overexpression of c-MYC kills glioma cells. TRAIL enhances cell death caused by c-MYC overexpression. **(C)** Combination of enzastaurin with carboplatin results in significantly reduced tumor volume in a mouse subcutaneous U87 xenograft model. **(D)** Combination of enzastaurin with carboplatin prolongs survival in U87 intracranial xenograft model.